



Brain targeting by intranasal drug delivery (INDD): a combined effect of trans-neural and para-neuronal pathway

Gulam Mustafa, Abdulmohsen H. Alrohaimi, Aseem Bhatnagar, Sanjula Baboota, Javed Ali & Alka Ahuja

To cite this article: Gulam Mustafa, Abdulmohsen H. Alrohaimi, Aseem Bhatnagar, Sanjula Baboota, Javed Ali & Alka Ahuja (2016) Brain targeting by intranasal drug delivery (INDD): a combined effect of trans-neural and para-neuronal pathway, *Drug Delivery*, 23:3, 923-929, DOI: [10.3109/10717544.2014.923064](https://doi.org/10.3109/10717544.2014.923064)

To link to this article: <http://dx.doi.org/10.3109/10717544.2014.923064>



Published online: 24 Jun 2014.



Submit your article to this journal [↗](#)



Article views: 227



View related articles [↗](#)



View Crossmark data [↗](#)

RESEARCH ARTICLE

Brain targeting by intranasal drug delivery (INDD): a combined effect of trans-neural and para-neuronal pathwayGulam Mustafa^{1,2}, Abdulmohsen H. Alrohaimi^{1,2}, Aseem Bhatnagar³, Sanjula Baboota¹, Javed Ali¹, and Alka Ahuja⁴¹Department of Pharmaceutics, Faculty of Pharmacy, Hamdard University, New Delhi, India, ²College of pharmacy, Al-Dawadmi Campus, Shaqra University, Riyadh, Kingdom of Saudi Arabia, ³Department of Nuclear Medicine Division (NMD), Institute of Nuclear Medicine & Allied Sciences, Timarpur, Timarpur, Delhi, India, and ⁴Department of Pharmacy, Oman Medical College, Azaiba, Muscat, Sultanate of Oman**Abstract**

The effectiveness of intranasal drug delivery for brain targeting has emerged as a hope of remedy for various CNS disorders. The nose to brain absorption of therapeutic molecules claims two effective pathways, which include trans-neuronal for immediate action and para-neuronal for delayed action. To evaluate the contribution of both the pathways in absorption of therapeutic molecules and nanocarriers, lidocaine, a nerve-blocking agent, was used to impair the action potential of olfactory nerve. An anti-Parkinson drug ropinirole was covalently complexes with ^{99m}Tc in presence of SnCl₂ using in-house developed reduction technology. The radiolabeled formulations were administered intranasally in lidocaine challenged rabbit and rat. The qualitative and quantitative outcomes of neural and non-neural pathways were estimated using gamma scintigraphy and UHPLC-MS/MS, respectively. The results showed a significant ($p \leq 0.005$) increase in radioactivity counts and drug concentration in the brain of rabbit and rat compared to the animal groups challenged with lidocaine. This concludes the significant contribution ($p \leq 0.005$) of trans-neuronal and para-neuronal pathway in nose to brain drug delivery. Therefore, results proved that it is an art of a formulator scientist to make the drug carriers to exploit the choice of absorption pathway for their instant and extent of action.

Introduction

In the last few decades, the importances of intranasal route (INDD) for delivering therapeutics to the brain for CNS and related disorders have gain much attention by many researchers all over the globe. The olfactory pathway, which shunts the blood brain barrier (BBB) (Mathison et al., 1998) and provide the shortest pathway between nasal cavities to brain leading to immediate action. The BBB may provide an easy access to the few lipophilic molecules ($MW \leq 500$ Da) but in most of the instances, it restricts the inflow of even lipophilic ($MW \geq 500$ Da) and most of the hydrophilic molecules after oral, transdermal and i.v. administration. Based on research works, the hypothesis of olfactory and trigeminal pathway came in existence which support nose to brain delivery (Mathison et al., 1998; Thorne & Frey, 2001; Mustafa et al., 2012a). The unique anatomy of olfactory region like large surface area, porous endothelial membrane, profound vascularization, lack of BBB and the shortest pathway make INDD, a highly unique for brain delivery with minimum drug related systemic side effects

Keywords

Brain targeting, gamma scintigraphy, intranasal drug delivery, neural pathway, non-neural pathway, olfactory nerve, ropinirole, trigeminal nerve

History

Received 30 March 2014
Revised 7 May 2014
Accepted 7 May 2014

(Turker et al., 2004). To date, lot of work has been reported for brain targeting using intanasal route (Mathison et al., 1998; Stevens et al., 2011). Few of them include nerve growth factor (Chou & Donovan, 1998), inorganic mercury (Henriksson & Tjalve, 1998), dihydroergotamine (Wang et al., 1998), taurine (Brittebo & Eriksson, 1995), carboxylic acids (Eriksson et al., 1999), 2',3'-didehydro-3'-deoxythymidine (Yajima et al., 1998) and many high molecular weight peptides (Frey et al., 1997) bagged in INDD. Kumar et al. (1982) who showed that progesterone ($MW \leq 314.46$ Da) achieved a higher distribution in the CSF than in the blood after intranasal administration. Similarly, Sakane et al. (1991) proved that lipid solubility of small molecules is directly proportional to the absorption from the nose to brain. Both the olfactory and trigeminal nerves innervate the nasal cavity, providing a direct connection with the brain (Shipley, 1985; Balin et al., 1986; Mathison et al., 1998). The intranasally administered therapeutic molecules get direct access to the brain via shunting BBB is widely accepted hypothesis (Merkus and van den Berg, 2007; Wen, 2011). However, selecting the INDD is not an easy target because of the nasal metabolizing enzymes and mucociliary clearance. Several metabolizing enzymes present in the nasal cavity such as cytochrome P-450 enzyme isoforms, carboxyl esterases and glutathione S-transferases which might play an inhibitory role for INDD

Address for correspondence: Dr. Alka Ahuja, Professor, Department of Pharmacy, Oman Medical College, P.O. 620, P.C. 130, Azaiba, Muscat, Sultanate of Oman. Tel: +966594429769. Email: alkaahuja@yahoo.com, gulampharma@gmail.com

(Aceto et al., 1989; Lewis et al., 1994). Similarly, the nasal epithelium is covered by a mucus layer (pH, 5.5–6.5), may entrap particles and gets cleared from nasal cavity by the ciliary movement (clearance time ≤ 20 min) as mentioned in earlier reports (Mustafa et al., 2012a). Hence, for effective INDD, a suitable carrier with mucoadhesion property is pre-requisite (Felt et al., 1998; Illum, 1998; Agnihotri et al., 2004; Yao et al., 2008). Therefore, a successful study was designed to investigate drug transport from nose to brain using mucoadhesive-coated nanocarriers (Mustafa et al., 2012a, 2013a). However, the effective nose to brain absorption of therapeutic molecules claims two significant pathways, which include trans-neuronal for immediate action and para-neuronal for delayed action. Therefore, present study was design to test this hypothesis of trans-neural and para-neural pathway in nose to brain targeting using lidocaine a nerve desensitizer. For qualitative and quantitative estimation of therapeutic molecules, gamma scintigraphy (Mustafa et al., 2013a) and UHPLC-MS/MS (Mustafa et al., 2012b) were used in this study.

Materials and methodology

Chemicals

A gift sample of ropinirole (ROP) was obtained from Wockhardt Pharmaceutical, Aurangabad, India. Propylene glycol mono caprylic ester (Sefsol 218[®]) was gift sample from Nikko Chemicals (Tokyo, Japan). Medium chain triglyceride (Labrafac[®]), caprylo caproyl macrogol-8-glyceride (Labrasol[®]), diethylene glycol monoethyl ether (Transcutol[®]) and polyglyceryl-6-dioleate (Plurol oleique[®]) were gift samples from Gattefosse (Saint Priest, Cedex France). Isopropyl myristate (IPM), glycerol triacetate (Triacetin), castor oil, polyoxyethylene sorbitan monooleate (Tween-80), PEG 200 and 400, propylene glycol, HPLC-grade methanol, acetonitrile and ammonium acetate were purchased from E-Merck (Mumbai, India). Stannous chloride dihydrate ($\text{SnCl}_2 \cdot 2\text{H}_2\text{O}$) were purchased from Sigma Chemical Company, St. Louis, MO. Sodium pertechnetate, separated from molybdenum-99 ($^{99\text{m}}\text{Tc}$) by solvent extraction method, was provided by Regional Center for Radiopharmaceutical Division (Northern Region), Board of Radiation and Isotope Technology, New Delhi, India. Deionized water was purified using a Milli-Q water purification system (Millipore, Bedford, MA).

Methodology

UHPLC-MS/MS analysis

UHPLC-MS/MS was performed with a Waters ACQUITY UHPLC[™] system (Serial No# F09 UPB 920M; Model Code# UPB; Waters Corp., Milford, MA) equipped with a binary solvent delivery system, auto-sampler, column manager and a tunable MS detector (Serial No# JAA 272; Synapt; Waters, Manchester, UK). Chromatographic separation was performed on a Waters ACQUITY UPLC[™] BEH C8 (100.0 mm \times 2.1 mm; 1.7 μm) column at $40 \pm 5^\circ\text{C}$. A reported UHPLC analysis with mobile phase consisted of acetonitrile–20 mM ammonium acetate (20:80; %v/v) was used for the present study (Mustafa et al., 2012b). The flow rate of the mobile phase was kept at $0.250 \text{ ml min}^{-1}$ with a run time of

2.0 min. Quantitation was performed using electron spray ionization (ESI) with ms scane m/z 261.2 \rightarrow 160 (ropinirole) and m/z 325 \rightarrow 262 (escitalopram, IS), respectively.

Ethical approval

Healthy New Zealand white rabbit weighing 2.5–3 kg was chosen for scintigraphic imaging. The study was designed after receiving approval from Animal Ethical Committee, Jamia Hamdard, New Delhi, India, and confirms to National guidelines on the care and use of laboratory animals (protocol proposal no: 729/2010). Similarly, Sprague–Dawley weighing 200–250 g were chosen for quantitative estimation and acclimatized to laboratory conditions. An approval (protocol proposal no: 745/2011) from Animal Ethical Committee, Jamia Hamdard, New Delhi, was taken. Normal food and water was provided *ad libitum*. The temperature of the animal room was kept at 22°C ($\pm 3^\circ\text{C}$) with relative humidity maintained at $65 \pm 0.5\%$ throughout the experiment.

Radiolabeling protocol

The molecules of ropinirole was covalently complexed with $^{99\text{m}}\text{Tc}$ in the presence of stannous chloride dihydrate ($\text{SnCl}_2 \cdot \text{H}_2\text{O}$) by using established reduction based technology developed by the Institute of Nuclear Medicine and allied Sciences (INMAS), Delhi, India (Mustafa et al., 2012a, 2013a). In brief, ROP solution was mixed with stannous chloride dihydrate (1:1) solution (100 mg in 100 ml of 0.10 N HCl) with continuous shaking. The pH was adjusted to 7.0 ± 0.5 using 50 mM sodium bicarbonate solution. To the resultant mixture was exposed to $^{99\text{m}}\text{Tc}$ -pertechnetate (75–400 MBq) over a period of 1 min with continuous mixing. The total exposure was monitored in Gama counter. In case of insufficient radio counts, the resultant solution was again exposed to the $^{99\text{m}}\text{Tc}$ -pertechnetate chamber. Now, the resultant mixture was incubated ($30 \pm 0.5^\circ\text{C}$) for 30 min in an inert environment. The final volume was made up using isotonic (0.90% w/v) saline solution. The radiochemical purity of $^{99\text{m}}\text{Tc}$ -ROP solution ($^{99\text{m}}\text{Tc}$ -labeled ROP) was determined by instant thin-layer chromatography (ITLC; Gelman Sciences, Inc, Ann Arbor, MI) using a previously optimized mobile phase consisting of acetone (100% v/v). The effect of incubation time, pH and stannous chloride concentration on radiolabeling efficiency were studied to achieve optimum reaction conditions. The radiolabeling efficiency of ropinirole with $^{99\text{m}}\text{Tc}$ was also characterized based on serum and saline stability up to 24 h as per previously reported methods using a gamma counter (Capintec, Ramsey, NJ) (Md et al., 2012; Mustafa et al., 2012a).

Preparation of nanoemulsion

The radiolabeled ropinirole was converted into nanoemulsion formulation ($^{99\text{m}}\text{Tc}$ -NE_{ROP}) using water titration technique as already discussed in our previous research (Mustafa et al., 2009, 2012c). In brief, surfactant and cosurfactant were mixed in different volume ratios (1:0, 1:1, 1:2, 1:3, 2:1, 3:1 and 4:1) to construct different phase diagram. Similarly, radiolabeled ROP predissolved in oil was mixed with specific surfactant:cosurfactant (Smix) ratios (1:9, 2:8, 3:7, 4:6, 5:5, 6:4, 7:3, 8:2 and 9:1) in separate glass vials. Slow titration of each

combination of oil and Smix was performed with water and visual inspections were made after each addition. The physical state of the mixture was marked on the ternary phase diagrams with axes representing aqueous phase, oil phase and Smix phase, respectively. Now, from each phase diagrams, different composition were selected and was screen on the basis of thermodynamic stability and dispersebility as already discussed in our earlier article (Talegaonkar et al., 2009; Mustafa et al., 2009, 2012c). The formulations obtained were further screened in sequence starting from *in vitro* release, particle size distribution, zeta potential, transmission electron microscopy and finally by *ex vivo* permeation using porcine nasal mucosa (Mustafa et al., 2012c). In a study, the optimized nanoemulsion showed certain limitation in intranasal administration as discussed in my previous report (Mustafa et al., 2012a). The inability was limited drug residence time and insufficient mucoadhesion. Therefore, chitosan were premixed with the optimized self-nanoemulsifying mixture to coat the nanoemulsion surface (Mustafa et al., 2013a, Calvo et al., 1997).

Lipophilicity

The partition coefficient of the optimized formulation was determined by ‘‘Shake flask method’’. Equal volume of chloroform and distilled water was taken in a conical flask and the formulations containing ROP (NE_{ROP}) was added. This mixture was kept in a mechanical shaker at 100 rpm for 1 h. The mixture was removed from the mechanical shaker, transferred into a separating funnel and then allowed to stand for 24 h in order to separate the two distinct solvent layers. The solvent layers were separated with the help of separating funnel, filtered, diluted and ROP content was estimated by UHPLC-MS/MS.

Animal experimental design for scintigraphy imaging

Three New Zealand white rabbits for each formulations ($n = 3$; male; 2–3 months old; 2.5–3.0 kg) per time point were used for gamma-scintigraphy imaging for qualitative study. Similarly, Sprague–Dawley rats ($n = 3$) weighing between 200 and 250 g were selected for quantitative estimation of intranasally administered ropinirole. Experimental animals were divided into four groups which include treatment group (Group A) pretreated with saline (Group A), i.e. 0.0% v/v lidocain, treatment group (Group B) pretreated with 0.25% v/v lidocain, treatment group (Group C) pretreated with 0.5% v/v lidocain and treatment group (Group D) pretreated with 1.0% v/v lidocain treated. After 30 min of pretreatment with lidocain, all groups were given $^{99m}\text{Tc-NE}_{ROP}$ through intranasal route. The radiolabeled drug formulation, $^{99m}\text{Tc-NE}_{ROP}$ (200 $\mu\text{Ci}/100 \mu\text{l}$) containing 200 μg Rop (equivalent to 1000 $\mu\text{g}/\text{kg}$ body weight) was administered in each nostril with the help of soft catheter fitted to a 25- μl Hamilton microsyringe. The rabbits were placed on board and images were captured using single positron emission computerized tomography (SPECT), provided by GE healthcare system (Hawkeye Millennium VG, GE Medical Systems, Milwaukee, WI) and the images were recorded using the eNTEGRA software (Milwaukee, WI) (Milwaukee, WI, USA) at proposed time intervals. Similarly, in case of rats, 1 h after

treatment animals were killed and the blood and brain were collected. The radioactivity present in brain and blood was measured using non-shielding well-type gamma scintillation counter (Capintec, well counter, Ramsey, NJ).

Quantification in brain by UHPLC-MS/MS

After estimating the radioactivity counts, brains were homogenized (1:10) in phosphate buffer (pH 7.4, 10% w/v) and further centrifuged (5000 rpm, 30-min REMI Equipments, Delhi). The supernatant was separated and the proteins were further precipitated with Perchloric acid (12% v/v). The ropinirole present in the supernatant was extracted using ethyl acetate (liquid–liquid extraction). The procedure was repeated with remaining precipitate to extract out the possible traces of ropinirole and stored it in deepfreeze (-80°C). On the day of quantification, equal volume of internal standard (10 ng/ml escitalopram) was mixed in different samples after appropriate dilution. The samples (10 μl) were injected with auto sampler attached with UHPLC-MS/MS instrument, and the chromatogram of the same was produced to get the amount of ropinirole in the brain and plasma, respectively, using established method (Mustafa et al., 2012).

Results

Radiolabeling protocol

Radiolabeling of ropinirole was performed using in-house developed (INMAS, New Delhi, India) technique (Mustafa et al., 2012a) and their binding efficiency was estimated by gamma counter (Capintec) as shown in Table 1. The radiolabeled-ropinirole ($^{99m}\text{Tc-ROP}$) was used to prepare the nanoemulsion formulation ($^{99m}\text{Tc-NE}_{ROP}$) using the optimization table, and the maximum labeling efficiency determined after 24 h was found to be $95.15 \pm 1.31\%$ and $96.23 \pm 2.33\%$ after 0.5 h whereas $98.04 \pm 1.56\%$ and $96.19 \pm 4.15\%$ after 24 h in saline and rat serum, respectively. The maximum tagging ($98.76 \pm 1.25\%$) in saline solution was achieved after 1 h whereas in rat serum the maximum tagging ($98.11 \pm 1.85\%$) was achieved after 3 h. The binding efficiency showed that, gamma count could also be used for quantitative analysis.

Table 1. Radiolabeling stability in normal saline (0.9% w/v) and rat serum.

Time (h)	Percentage stability of $^{99m}\text{Tc-NE}_{ROP}$	
	0.9% NaCl	Rat serum
0.5	95.15 ± 1.31	96.23 ± 2.33
1	98.76 ± 1.25	97.49 ± 1.46
2	97.93 ± 1.64	97.66 ± 3.59
3	98.12 ± 1.58	98.11 ± 1.85
4	98.45 ± 1.96	97.58 ± 1.68
5	98.57 ± 1.44	97.34 ± 2.56
22	97.98 ± 2.72	97.15 ± 3.79
24	98.04 ± 1.56	96.19 ± 4.15

Ropinirole nanoemulsion radiolabeled with technetium ($^{99m}\text{Tc-NE}_{ROP}$).

Table 2. Partitioning potential of the optimized formulation in chloroform/water and chloroform/phosphate buffer (pH 5.6 and 7.4) mixture showing the impact of droplet size on its lipophilicity.

Partitioning medium	%Ropinirole partition in chloroform layer							
	NE_{ROP1}	NE_{ROP2}	NE_{ROP3}	NE_{ROP4}	NE_{ROP5}	NE_{ROP6}^{**}	NE_{ROP7}	$Soln^{ROP}$
Distilled water–chloroform	81.49 ± 3.59	73.66 ± 11.14	72.51 ± 3.64	77.94 ± 6.40	90.30 ± 2.62	95.67 ± 2.00	55.62 ± 8.81	8.38 ± 3.13
Phosphate buffer (5.6)–chloroform	83.12 ± 6.49	72.84 ± 7.73	70.36 ± 9.16	76.46 ± 7.93	88.53 ± 4.15	94.39 ± 3.93	56.97 ± 6.49	10.54 ± 2.95
Phosphate buffer (7.4)–chloroform	81.85 ± 8.75	65.79 ± 7.89	68.19 ± 5.34	71.81 ± 11.27	89.81 ± 2.91	95.09 ± 2.99	61.78 ± 3.21	13.46 ± 2.11

Decreasing order of droplet size of different formulations (Mustafa et al., 2012): $NE_{ROP7} \geq NE_{ROP2} \geq NE_{ROP3} \geq NE_{ROP4} \geq NE_{ROP1} \geq NE_{ROP5} \geq NE_{ROP6}$.

Decreasing order of partition co-efficient of different formulations: $NE_{ROP6} \geq NE_{ROP5} \geq NE_{ROP1} \geq NE_{ROP4} \geq NE_{ROP3} \geq NE_{ROP2} \geq NE_{ROP7}$.

Decreasing order of surface charge of different formulations (Mustafa et al., 2012): $NE_{ROP6} \geq NE_{ROP7} \geq NE_{ROP4} \geq NE_{ROP2} \geq NE_{ROP3} \geq NE_{ROP1} \geq NE_{ROP5}$.

The statistical significant difference for each formulation was calculated by student's *t*-tests: **p* < 0.05, ***p* < 0.005.

Table 3. Comparative systemic to brain counts of intranasally administered ^{99m}Tc -CSNE_{ROP} containing nerve blocking agents.

Specifications	Brain/systemic ratio (in terms of radioactivity counts)						
	5 min	10 min	15 min	30 min	45 min	60 min	
^{99m}Tc -CSNE _{ROP}							
0	$16.95 \pm 1.89 \times 10^{-2}$	$25.65 \pm 6.75 \times 10^{-2}$	$34.03 \pm 15.4 \times 10^{-2**}$	$19.96 \pm 3.27 \times 10^{-2}$	$7.27 \pm 2.04 \times 10^{-2}$	$3.16 \pm 0.67 \times 10^{-2}$	
0.25	$9.51 \pm 2.56 \times 10^{-2*}$	$8.24 \pm 1.92 \times 10^{-2}$	$7.96 \pm 2.6 \times 10^{-2}$	$8.19 \pm 6.62 \times 10^{-2}$	$2.69 \pm 1.36 \times 10^{-2}$	$1.29 \pm 0.43 \times 10^{-2}$	
0.5	$6.154 \pm 1.99 \times 10^{-2}$	$4.64 \pm 0.96 \times 10^{-2}$	$5.25 \pm 0.97 \times 10^{-2}$	$5.09 \pm 1.48 \times 10^{-2}$	$2.14 \pm 0.53 \times 10^{-2}$	$1.26 \pm 0.31 \times 10^{-2}$	
1.0	$0.74 \pm 0.22 \times 10^{-2}$	$0.94 \pm 0.26 \times 10^{-2}$	$0.91 \pm 0.18 \times 10^{-2}$	$0.107 \pm 0.44 \times 10^{-2}$	$0.039 \pm 0.02 \times 10^{-2}$	$0.021 \pm 0.014 \times 10^{-2}$	

The gamma scintigraphic study for determining the qualitative distribution profile was done using New Zealand white rabbit. Here, ^{99m}Tc -CSNE_{ROP} represents chitosan-coated ropinirole nanoemulsion radiolabeled with technetium.

The statistical significant difference at each time point was calculated by student's *t*-tests: **p* < 0.05, ***p* < 0.005.

Nanoemulsification

After constructing phase diagrams, different possible compositions were selected and screened on their thermodynamic performance, a detailed account has been discussed in our previous report (Mustafa et al., 2009, 2012c). The mean droplet sizes of different optimized formulations were 69.8 ± 9.08 nm (NE_{ROP1}), 98.1 ± 5.19 nm (NE_{ROP2}), 86.8 ± 7.35 nm (NE_{ROP3}), 74.61 ± 5.35 nm (NE_{ROP4}), 67.81 ± 8.29 nm (NE_{ROP5}), 58.61 ± 5.18 nm (NE_{ROP6}) and 108.62 ± 2.32 nm (NE_{ROP7}), respectively. Electrokinetic potential of different formulations were also done to know the surface charge on the nanoglobules. The electrokinetic potential (ζ -potential) of NE_{ROP6} was found maximum (−33.40 mV) compared to other formulations. Decreasing order of electrokinetic potential in different optimized formulations were followed as NE_{ROP6} (−33.40 mV) ≥ NE_{ROP7} (−32.51) ≥ NE_{ROP4} (−31.4) ≥ NE_{ROP2} (−30.38) ≥ NE_{ROP3} (−29.57) ≥ NE_{ROP1} (−25.27) ≥ NE_{ROP5} (−25.06) (Mustafa et al., 2012c). The release profile was investigated in three different dialyzing media (distilled water, pH 6.5 phosphate buffer and pH 7.4 phosphate buffers) to know the role of pH in dissolution. The release results confirmed that nanoemulsion is independent by the pH of the dissolution medium. The highest release of 72.23 ± 9.56% was obtained in formulation NE_{ROP6} . The decreasing order of dissolution profile were NE_{ROP6} (72%) ≥ NE_{ROP5} (64%) ≥ NE_{ROP3} (58%) ≥ NE_{ROP2} (56%) ≥ NE_{ROP7} (54%) ≥ NE_{ROP1} (48%) ≥ NE_{ROP4} (42%). The optimized formulation NE_{ROP6} was coated by chitosan (^{99m}Tc - NE_{ROP6}) to increase the mucoadhesion (Singla and Chawla, 2001). A detail study was already published in my earlier report (Mustafa et al., 2013a). Thin coating layers

around the nanoemulsion droplet determined by transmission electron microscopy followed by gamma imaging in rabbit proved the successful coating.

Lipophilicity

Besides physicochemical property of the therapeutic molecules, the fate of nanocarriers also depends on the overall lipophilicity (Levin, 1980; Wils et al., 1994). The partitioning behavior of different nanocarriers in the octanol–water or chloroform–water system directly shows the absorption potential across the biological membrane. In the preset study, chloroform–water was used to check the lipophilicity of different NE_{ROP} formulations. The highest partition were obtained for NE_{ROP6} having droplet size 58.61 ± 5.18 nm whereas minimum distribution was obtained for NE_{ROP7} with a droplet size 108.62 ± 2.32 nm. The increasing order of partition were followed as $NE_{ROP7} \leq NE_{ROP2} \leq NE_{ROP3} \leq NE_{ROP4} \leq NE_{ROP1} \leq NE_{ROP5} \leq NE_{ROP6}$ (Table 2). Depending upon the partitioning results and droplet size, NE_{ROP6} was finally selected for intranasal administration to target brain.

Qualitative estimation using gamma scintigraphy

The in-house developed methodology showed 98.76 ± 1.25% radiolabeling in normal saline and 98.11 ± 1.85% in rat serum as already mentioned in my research articles (Mustafa et al., 2012a, 2013a). After administering the tagged formulation coupled with different strength of lidocaine (0.25–1.0% v/v), scintigraphic imaging was performed to see the effective role of neuronal and trans-neuronal pathway in nose to brain drug delivery. Gamma scintigraphic imaging showed a significant brain translocalization of ^{99m}Tc - NE_{ROP} in the rabbit treated

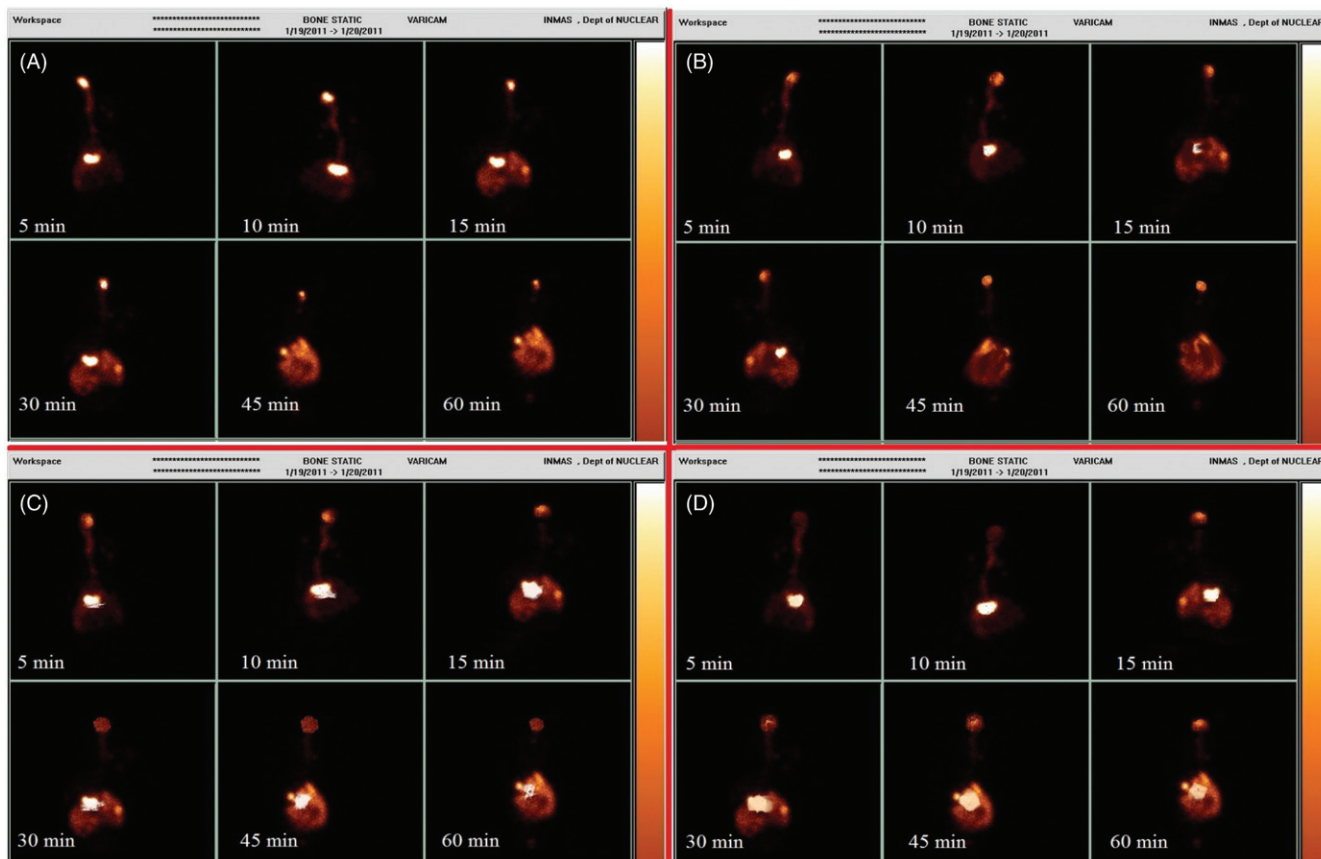


Figure 1. Gamma scintigraphic imaging showing impact of neuronal and non-neuronal pathway in nose to brain targeting after administering $^{99m}\text{Tc-NE}_{\text{ROP}}$ with different strengths of lidocaine as a nerve blocking agents. Here, treatment group (A) represent $^{99m}\text{Tc-NE}_{\text{ROP}}$ with lidocaine (0% v/v), group (B) $^{99m}\text{Tc-NE}_{\text{ROP}}$ with lidocaine (0.1% v/v), group (C) $^{99m}\text{Tc-NE}_{\text{ROP}}$ with lidocaine (0.2% v/v) and group (D) $^{99m}\text{Tc-NE}_{\text{ROP}}$ with lidocaine (0.3% v/v).

Table 4. Quantitative estimation of ropinirole in brain and blood after intranasal administration of CSNE_{ROP} containing lidocain as an olfactory nerve blocker.

Lidocain (%v/v)	Sampling time (h)	Concentration (ng/g)			
		0.5 h	1 h	6 h	24 h
0	Blood	$202.29 \pm 8.33 \times 10^{-3}^{**}$	$180.78 \pm 11.48 \times 10^{-3}$	$83.89 \pm 9.12 \times 10^{-3}$	$21.83 \pm 4.36 \times 10^{-3}$
	Brain	$18.96 \pm 2.53 \times 10^{-3}^{**}$	$14.74 \pm 1.08 \times 10^{-3}$	$6.58 \pm 1.03 \times 10^{-3}$	$1.56 \pm 0.91 \times 10^{-3}$
0.25	Blood	$155.61 \pm 11.24 \times 10^{-3}$	$134.11 \pm 9.77 \times 10^{-3}$	$68.21 \pm 3.49 \times 10^{-3}$	$18.34 \pm 2.95 \times 10^{-3}$
	Brain	$12.39 \pm 1.81 \times 10^{-3}^{*}$	$10.03 \pm 3.01 \times 10^{-3}$	$4.71 \pm 0.85 \times 10^{-3}$	$0.82 \pm 0.06 \times 10^{-3}$
0.5	Blood	$141.46 \pm 7.22 \times 10^{-3}$	$134.96 \pm 6.29 \times 10^{-3}$	$51.68 \pm 3.75 \times 10^{-3}$	$16.55 \pm 1.92 \times 10^{-3}$
	Brain	$10.56 \pm 2.19 \times 10^{-3}$	$8.13 \pm 0.95 \times 10^{-3}$	$2.3 \pm 0.59 \times 10^{-3}$	$0.38 \pm 0.10 \times 10^{-3}$
1.0	Blood	$109.76 \pm 8.79 \times 10^{-3}$	$82.03 \pm 4.21 \times 10^{-3}$	$38.79 \pm 5.26 \times 10^{-3}$	$11.91 \pm 2.14 \times 10^{-3}$
	Brain	$9.33 \pm 2.62 \times 10^{-3}$	$6.58 \pm 2.05 \times 10^{-3}$	$1.15 \pm 0.06 \times 10^{-3}$	$0.16 \pm 0.05 \times 10^{-3}$

The radioactivity was measured per gram of organ, while in LC-MS/MS data are shown in nanogram per gram (ng/g) sample (mean \pm SD, $n = 3$). Any significant difference at each time point was calculated according to the Student's t -tests: $^{*}p < 0.005$, $^{**}p < 0.001$.

with the formulation devoid of lidocaine. The dynamic modeling showed a geometrical decrease of $^{99m}\text{Tc-NE}_{\text{ROP}}$ localization in the brain of rabbit upon increasing the lidocaine contribution in the formulation (Table 3). In Figure 1, scintigraphic imaging concluded that, the region of interest (Brain) showed high accumulation of radioactivity in contrast to the peripheral organ that confirms brain targeting potential of intranasal route. The same study was repeated in rats to further authenticate the role of neuronal and trans-neuronal pathway by quantitative method using UHPLC-MS/MS.

Quantitative estimation using gamma scintigraphy and UHPLC-MS/MS

The result obtained in rat was quantitated further by gamma counting and UHPLC-MS/MS data (Tables 3 and 4). The amount of ropinirole in brain of rat treated with $^{99m}\text{Tc-NE}_{\text{ROP}}$ with 0% lidocaine was found to be $23\,655.76 \pm 5173.51$ pg/g where 8559.21 ± 2334.67 pg/g of ropinirole in brain treated with $^{99m}\text{Tc-NE}_{\text{ROP}}$ dissolved in 1.0% lidocaine. The gamma counts further potentiate the finding (Figure 1).

Discussion

Tagging stability in plasma proteins was done for 24 h as already shown in our published research article (Mustafa et al., 2012a). This finding suggested that, qualitative estimation in terms of ^{99m}Tc counts would give an indirect estimation of ropinirole. The maximum tagging even after 24 h was found to be $98.04 \pm 1.56\%$ and $96.19 \pm 4.15\%$, respectively, in saline and rat serum. This showed that, serum protein did not interfere with the stability of $^{99m}\text{Tc-NE}_{\text{ROP}}$. The maximum drug release of $72.23 \pm 9.56\%$ was obtained in formulation $\text{NE}_{\text{ROP}6}$ which showed the significant role of droplet size and overall size distribution. In many instances, besides of lower droplet size distribution, even though the release profile was not appropriate. This may be because of high polydispersity index. The partitioning behavior of different formulations followed as $\text{NE}_{\text{ROP}6} \geq \text{NE}_{\text{ROP}5} \geq \text{NE}_{\text{ROP}1} \geq \text{NE}_{\text{ROP}4} \geq \text{NE}_{\text{ROP}3} \geq \text{NE}_{\text{ROP}2} \geq \text{NE}_{\text{ROP}7}$. If we compare the trends of droplet size and surface charge, then it seems to be very difficult to come to the final remarks. After comparative interpretation of different data (droplet size, surface charge and partition co-efficient) it was concluded that it is not only the lipophilicity which effect the partitioning behavior (Wils et al., 1994), but to some extent the size distribution and surface charge of the droplet in the resultant formulations decides the fate of absorption (Table 2). Results also approved that, nanoemulsion are independent of pH of partitioning medium as it is stabilized using non-ionic surfactants.

Gamma scintigraphic imaging showed the brighter spot as well as highest gamma counts in the brain in comparison to systemic organs as shown in Figure 1, corroborating the earlier report by Sakane et al. (1991). In lidocain-challenged animals, it was hypothesized after examining the effects of blocking action potential of the olfactory nerve (ON). The apparent stimulation and subsequent depression produced by applying local anesthetics to the CNS presumably were reported due to suppression of neuronal activity (Nattel et al., 1987; Brunton et al., 2008). The nerve blocking effects impaired the conduction of action potential in the olfactory nerve leading to the suppression of neuronal function (Stakic et al., 2011). The results showed that, there was a significant increase in radioactivity counts in the animal brain treated with $^{99m}\text{Tc-NE}_{\text{ROP}}$ with 0% lidocain ($p^* < 0.005$) compared to the rat brain treated with $^{99m}\text{Tc-NE}_{\text{ROP}}$ containing 0.25%, 0.5% and 1.0% lidocain (v/v) shown in Table 3. The decreasing order of the gamma count in the brain at first 5 min treated with $^{99m}\text{Tc-NE}_{\text{ROP}}$ formulations after challenging with different level of lidocain were $^{99m}\text{Tc-NE}_{\text{ROP}+0\%}$ lidocain ($19\,128.65 \pm 9588.43$ cps/g) \geq $^{99m}\text{Tc-NE}_{\text{ROP}+0.25\%}$ lidocain ($12\,707.87 \pm 5301.83$ cps/g) \geq $^{99m}\text{Tc-NE}_{\text{ROP}+0.5\%}$ lidocain (8923.13 ± 1085.57 cps/g) \geq $^{99m}\text{Tc-NE}_{\text{ROP}+1.0\%}$ lidocain (1124.67 ± 334.41 cps/g). Similarly, the decreasing order of systemic exposure of radioactivity with different $^{99m}\text{Tc-NE}_{\text{ROP}}$ formulations were $^{99m}\text{Tc-NE}_{\text{ROP}+1.0\%}$ lidocain ($151\,982.43 \pm 8519.54$ cps/g) \geq $^{99m}\text{Tc-NE}_{\text{ROP}+0.5\%}$ lidocain ($144\,997.23 \pm 6858.07$ cps/g) \geq $^{99m}\text{Tc-NE}_{\text{ROP}+0.25\%}$ lidocain ($133\,626.39 \pm 20\,710.27$ cps/g) \geq $^{99m}\text{Tc-NE}_{\text{ROP}+0\%}$ lidocain ($112\,853.39 \pm 5073.24$ cps/g). The systemic exposure results were obtained to be just reverse in comparison to the brain exposure. The results also

suggested that to prevent systemic exposure, an immediate absorption is always required through intranasal route. A significant high-radioactivity count (cps/g) was obtained in rat group that was not put under lidocain challenge compared to the treatment group challenged with different concentration of lidocain. This indicates the possibility of two functional pathways for drug absorption from olfactory region, i.e. neuronal (trans-neuronal) and non-neuronal (para-neuronal). When one pathway (neuronal pathway) was blocked using nerve desensitizer lidocain, the overall absorption in the brain region through combined neuronal and non-neuronal pathway was decreased leading to simultaneously increase in the systemic absorption. This result was further authenticated by quantitative estimation of ropinirole by UHPLC-MS/MS (Mustafa et al., 2012b), which corroborated with the gamma scintigraphy finding. These findings indicated that the lidocaine blocked a large number of ON axons is that the field potential could be blocked. A similar finding of field potential abolishment after lidocain administration was already reported by Stakic et al. (2011). The lidocain slows down the action potential of the ON leading to decrease contribution in absorption through olfactory tract and hence the lower radioactivity counts and ROP concentration in brain were observed. All these results potentiate the existence of neuronal (trans-neuronal) and non-neuronal (para-neuronal) pathway supported drug absorption by intranasal route. These findings are in good agreement with the previous literatures (Shipley, 1985; Mathison et al., 1998; Illum, 2000; Thorne & Frey, 2001; Yu et al., 2004).

Conclusion

Intranasal NE_{ROP} avoid the first-pass metabolism, protect therapeutic molecules from nasal metabolizing enzymes and circumvent the BBB, which markedly improve brain bioavailability. Study somehow able to prove the presence of neuronal (trans-neuronal) and non-neuronal (para-neuronal) pathways being used in intranasal absorption. Intranasal route might be helpful for both increasing brain therapeutic levels and simultaneously reducing systemic unwanted consequences of ropinirole. The effectiveness of the lipidic carrier over hydrophilic carriers based formulations cannot be ignored while going for the INDD. Finally, intranasal delivery engineered with certain carrier may facilitate the treatment and prevention of many different neurologic and psychiatric disorders after intranasal administration.

Acknowledgements

The authors are thankful to Wockhardt Pharmaceutical (Aurangabad, India), Gattefosse (Saint Priest, Cedex France) and Nikko chemical Ltd (Tokyo, Japan) for providing ropinirole, Transcutol and sefsol 218, respectively. The authors are also grateful to Director, Institute of Nuclear Medicine and Allied Sciences for providing facilities to carry out *in vivo* experiments on animal models.

Declaration of interest

The authors report no conflicts of interest. The authors alone are responsible for the content and writing of the article.

The authors are thankful to the Council for Scientific and Industrial Research (CSIR), Pusa road, New Delhi, for the grant, which supported this study.

References

- Aceto A, Dillio C, Angelucci S, et al. (1989). Glutathione transferases in human nasal mucosa. *Arch Toxicol* 63:427–31.
- Agnihotri SA, Mallikarjuna NN, Aminabhavi TM. (2004). Recent advances on chitosan based micro-and nanoparticles in drug delivery. *J Control Rel* 100:5–28.
- Balin BJ, Broadwell RD, Salzman M, El-Kalliny M. (1986). Avenues for entry of peripherally administered protein to the central nervous system in mouse, rat, and squirrel monkey. *J Comp Neurol* 251:260–80.
- Brittebo EB, Eriksson C. (1995). Taurine in the olfactory system: effects of the olfactory toxicant dichlobenil. *Neurotoxicology* 16:271–80.
- Brunton LL, Lazo JS, Parker EL. (2008). Local anaesthetic. Goodman & Gilman's the pharmacological basis of therapeutics. 11th ed. OH, USA: The MacGraW-Hill Companies.
- Calvo P, Remunan C, VilaJato JL, Alonso MJ. (1997). Development of positively charged colloidal drug carriers: chitosan-coated polyester nanocapsule and submicron emulsions. *Colloid Polym Sci* 275:46–53.
- Chou KJ, Donovan MD. (1998). The distribution of local anaesthetics into the CSF following intranasal administration. *Int J Pharm* 168: 137–45.
- Eriksson C, Bergman U, Franzen A, et al. (1999). Transfer of some carboxylic acids in the olfactory system following intranasal administration. *J Drug Target* 7:131–42.
- Felt O, Buri P, Gurny R. (1998). Chitosan: a unique polysaccharide for drug delivery. *Drug Dev Ind Pharm* 24:979–93.
- Frey WH, Liu J, Chen X, et al. (1997). Delivery of 125I-NGF to the brain via the olfactory route. *Drug Deliv* 4:87–2.
- Henriksson J, Tjalve H. (1998). Uptake of inorganic mercury in the olfactory bulbs via olfactory pathways in rats. *Environ Res* 77:130–40.
- Illum L. (1998). Chitosan and its use as a pharmaceutical excipient. *Pharm Res* 15:1326–31.
- Illum L. (2000). Transport of drugs from the nasal cavity to the central nervous system. *Eur J Pharm Sci* 11:1–18.
- Kumar TCA, David GF, Sankaranarayanan A, et al. (1982). Pharmacokinetics of progesterone after its administration to ovariectomized rhesus monkeys by injection, infusion, or nasal spraying. *Proc Natl Acad Sci USA* 79:4185–9.
- Levin VA. (1980). Relationship of octanol/water partition coefficients and molecular weight to rat brain capillary permeability. *J Med Chem* 23:682–4.
- Lewis JL, Nikula KJ, Novak R, Dahl AR. (1994). Comparative localization of carboxyl esterase in F344 rat, beagle dog and human nasal tissue. *Anat Rec* 239:55–64.
- Mathison S, Nagilla R, Kompella UB. (1998). Nasal route for direct delivery of solutes to the central nervous system: fact or fiction. *J Drug Target* 5:415–41.
- Merkus FW, van den Berg MP. (2007). Can nasal drug delivery bypass the blood-brain barrier?: questioning the direct transport theory. *Drugs R D* 8:133–44.
- Mustafa G, Ahmad N, Baboota S, et al. (2012b). Stressed kinetics of nanoemulsion formulation encapsulated ropinirole with a validated ultra high performance liquid chromatography/synapt mass spectrometry (UPLC-MS/MS ESI-Q-TOF). *J Chin Chem Soc* 59:1021–30.
- Mustafa G, Baboota S, Ahuja A, Ali J. (2012c). formulation development of chitosan coated intra nasal ropinirole nanoemulsion for better management option of parkinson: an in vitro ex vivo evaluation. *Current Nanoscience* 8:348–60.
- Mustafa G, Baboota S, Ali J, et al. (2013) Nose to Brain targeting potential of a chitosan coated nanoformulation: Pharmacodynamic and Pharmacoscintigraphic evaluation. *Sci Adv Mat* 5:1236–49.
- Mustafa G, Khan ZI, Bansal T, Talegaonkar S. (2009). Preparation and characterization of oil in water nano-reservoir systems for improved oral delivery of atorvastatin. *Curr Nano Sci* 5:428–40.
- Mustafa G, Kumar N, Singh T, Baboota et al. (2012a) Effect of homogenization on the fate of true nanoemulsion in brain translocation: a gamma scintigraphic evaluation. *Sci Ad Material* 4:739–48.
- Nattel S, Gagne G, Pineau M. (1987). The pharmacokinetics of lignocaine and -adrenoceptor antagonists in patients with acute myocardial infarction. *Clin Pharmacokinet* 13:293–316.
- Sakane T, Akizuki M, Yamashita S, et al. (1991). The transport of a drug to the cerebrospinal fluid directly from the nasal cavity: the relation to the lipophilicity of the drug. *Chem Pharm Bull* 39: 2456–8.
- Shiple MT. (1985). Transport of molecules from nose to brain: transneuronal anterograde and retrograde labeling in the rat olfactory system by wheat germ agglutinin-horseradish peroxidase applied to the nasal epithelium. *Brain Res Bull* 15:129–42.
- Singla AK, Chawla M. (2001). Chitosan: some pharmaceutical and biological aspects-an update. *J Pharm Pharmacol* 53:1047–67.
- Stakic J, Suchanek JM, Ziegler GP, Griff ER. (2011). The source of spontaneous activity in the main olfactory bulb of the rat. *PLoS ONE* 6:e23990.
- Stevens J, Ploeger BA, van der Graaf PH, et al. (2011). Systemic and direct nose-to-brain transport pharmacokinetic model for remoxipride after intravenous and intranasal administration. *Drug Metab Dispos* 39:2275–82.
- Talegaonkar S, Mustafa G, Akhter S, Iqbal ZI. (2009). Design and development of oral oil-in-water nanoemulsion formulation bearing atorvastatin: in vitro assessment. *J Disp Sci Tech* 30:1–12.
- Thorne RG, Frey WH. (2001). Delivery of neurotrophic factors to the central nervous system. *Clin Pharma* 40:907–46.
- Turker S, Onur E, Ozer Y. (2004). Nasal route and drug delivery systems. *Pharm World Sci* 26:137–42.
- Wang Y, Aun R, Tse FLS. (1998). Brain uptake of dihydroergotamine after intravenous and nasal administration in the rat. *Biopharm Drug Dispos* 19:571–5.
- Wen MM. (2011). Olfactory targeting through intranasal delivery of biopharmaceutical drugs to the brain: current development. *Discov Med* 11:497–503.
- Wils P, Warnery A, Phung-Ba V, et al. (1994). High lipophilicity decreases drug transport across intestinal epithelial cells. *J Pharmacol Exp Ther* 269:654–8.
- Yajima T, Juni K, Saneyoshi M, et al. (1998). Direct transport of 2',3'-didehydro-3'-deoxythymidine (D4T) and its ester derivatives to the cerebrospinal fluid via the nasal mucous membrane in rats. *Biol Pharm Bull* 21:272–7.
- Yao J, Zhou JP, Ping QN, et al. (2008). Distribution of nobiletin chitosan-based microemulsions in brain following i.v. injection in mice. *Int J Pharm* 352:256–62.
- Yu CR, Power J, Barnea G, et al. (2004). Spontaneous neural activity is required for the establishment and maintenance of the olfactory sensory map. *Neuron* 42:553–66.